8

Prediction of Wave Height Based on the Monitoring of Surface Wind

Tsukasa Hokimoto
Graduate School of Mathematical Sciences, The University of Tokyo
Japan

1. Introduction

The ocean wave is one of the physical factors which cause serious sea disasters, and its prediction provides the information available for various human activity related to the sea. More than a half-century has passed since original theories for wave hindcasting techniques have been proposed in the pioneering papers such as Sverdrup and Munk (1947) and Pierson, Neumann, and James (1960) and so on, the method and the technique for wave prediction problem have progressed a great deal, against the background of recent progresses in the technologies of measurement and computation. However, even at the present, the prediction of the wave phenomena is still a difficult problem, and the technology for wave prediction is going on further development. There are several reasons why the prediction of the phenomena related to the sea state is a difficult problem even now. One of the reasons is the complexity of the physical mechanism on the wave development. When the sea is getting rough by wind forcing, the sea surface movement is affected by the interactions among the meteorological factors, such as wind motion and atmospheric pressure, and the topographical influence which varies by region. It means that the theoretical description of the sea surface movement, taking into account of the dynamic relationship among these factors, is very complicated. And another reason is the difficulty of the field measurement at sea. It is often the case that we can not carry out constant monitoring on the necessary meteorological factors, due to the lack of measurement facilities, sudden malfunction of a measurement instrument, and so on.

In the traditional research on the wave prediction problem, various statistical methods for the prediction of the sea state data have been proposed until now. However, most of such methods have been considered based on the measured data obtained by buoys or ships. In Japan, the Japan Meteorological Agency has set up about 1300 regional stations for the ground-based meteorological monitoring, which is called Automated Meteorological Data Acquisition System (AMeDAS), throughout of this country, and over 80 sensors for ultrasonic wave height meters in the coastal areas. They provide measured data on wave height and various meteorological factors constantly, which are available via Internet. It is thought that the physical factors which make influence on the sea condition, such as the wind speed and wind direction, change with spatial and temporal correlations. So, as an approach to the above wave prediction problem, we develop a statistical model for predicting the change of wave height from the change of surface wind, obtained by constant ground-based observation.

In this chapter, we provide two topics on the statistical modeling for the prediction of wave height. The first topic is a modeling for predicting the change of wave height based on ocean wind, by applying the method proposed in our previous paper (Hokimoto and Shimizu (2008)). And the second topic is the development of a statistical model for predicting wave height, based on the change of surface wind, obtained by ground-based observation. Also, the effectiveness in prediction using the proposed models is examined by means of the numerical experiment.

The sections below are organized as follows. In the next section, we outline traditional researches on the statistical models for the sea state data. In section 3, we present a method for the wave height prediction based on the measurement of ocean wind. In section 4, we develop a model for predicting wave height based on the measurement of surface wind, obtained by ground-based observation. And section 5 provides a summary of the result and discussion of further research on this topic.

2. Time series models for the sea state analysis

It is well-known that the wave motion under low wind speed can be approximated by Gaussian process. For the measured data in this aspect, the linear stationary time series models proposed by Box and Jenkins (1976), such as autoregressive (AR) model or autoregressive moving average (ARMA) model, have been widely used to construct a predictor. In fact, various applications to wave height data (e.g., Cunha and Guedes (1999), Yim et. al. (2002)) and the wind data (e.g., Brown et. al. (1984), Daniel and Chen (1991)) have been reported by many authors.

However, as for the wave motion during the wave development process, the above stationary models do not give reasonable predictions. There are also many models which are applicable to the measured data in the transitional aspect. One is standard linear nonstationary time series models. For example, autoregressive integrated moving average (ARIMA) model (Box and Jenkins (1976)), the autoregressive model with time varying coefficients (Kitagawa and Gersch (1985)), and generalized autoregressive conditional heteroskedasticity (GARCH) model (Bollerslev (1986)) are used widely to the nonstationary time series data. Also, if the speed in changing statistical structure can be regarded to be slow, we can apply a stationary AR model to the time series data in the local time interval which can be regarded to be stationary. For example, a model for predicting the change of nonstationary spectral density function of the sea surface movement during the wave development process was developed based on this concept (Hokimoto et. al. (2003)). There are also nonstationary time series models based on the decomposition of the trend and the other components (e.g., Athanassoulis et. al. (1995), Stefanakos et. al. (2002), Walton and Borgman (1990)).

One of interests when we treat the measured data on the sea state is how we treat the directional time series data on the wind direction. This problem is serious when we consider a statistical model to the multivariate time series data including wave height, wind speed and wind direction, because directional data have a unique property that they take the values on the circle. In the framework of directional statistics, various methodologies for statistical inferences on the directional data have been proposed (for example, Mardia and Jupp (2000)). Among them, multivariate regression models, including circular and linear variables, have been often proposed in environment studies. Johnson and Wehrly (1978) considered the theoretical background of the linear parametric regression, which has the linear variable and the angular variable. And the extension of their model has given in Fisher and Lee (1992), SenGupta (2004), SenGupta and Ugwuowo (2006), and so forth. However, there have been

only limited attempts to model multivariate angular-linear data. In Hokimoto and Shimizu (2008), we developed an angular-linear time series model to express the dynamic structure among wave height, wind speed and wind direction, by extending the multiple regression model by Johnson and Wehrly (1978), and showed the effectiveness on wave height prediction between the change in ocean wind and the change in wave height. Our interest here is that the model whose structure is similar to the above model may be effective for the description of the dynamic relationship between wave height and surface wind.

3. Wave height prediction based on the change of ocean wind

In this section, we present a statistical method for predicting the change of wave height from the motion of ocean wind, based on Hokimoto and Shimizu (2008). The development of this method was motivated by the measured data obtained from ocean surveys using a research ship, in Hunka-bay, Hokkaido, Japan.

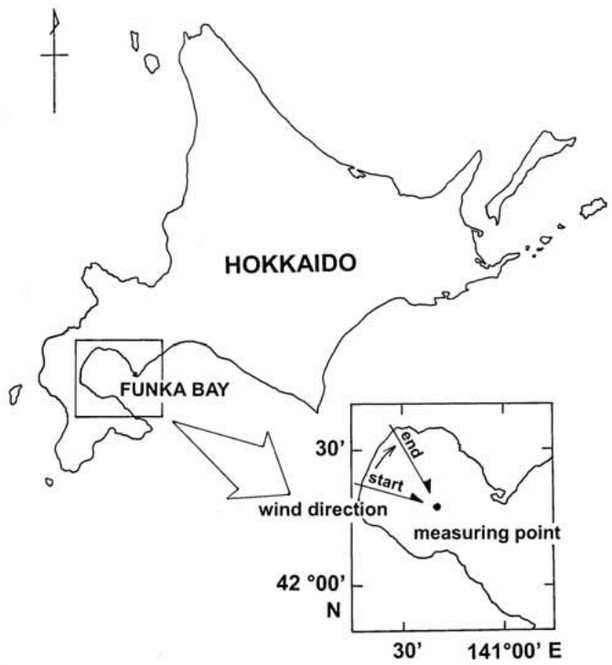

Fig. 1. A map around the measuring point

3.1 In-situ monitoring on wave height and ocean wind

Figure 1 shows a map around the measuring point (42°17′N, 140°40′E). We have measured the changes of relative sea surface level, wind speed and wind direction in Hunka-bay. For the relative sea surface movement, we measured relative displacement from the mean of the sea surface movement over 10 minutes by using an ultrasonic wave height meter of the research ship. Also, the changes in wind speed and wind direction at about 15 meters height from the sea surface were measured by using an ultrasonic wind meter. After the measurement, we obtained the time series data on 1/3 significant wave height, mean wind speed and mean wind direction for every 1 minute, based on the measured records.

Figure 2 displays the time series data obtained in the above, which were measured on Dec. 2, 1999. From the top, the significant wave height (m), the wind speed (m/s), and the wind

direction (rad.) are shown, where each sample size is 90. It is noted that the origin of the wind direction data is defined to be north and the positive value means the clockwise direction. According to the weather maps of the sampling day, as well as the days before and after, the location of atmospheric pressure formed typical pattern of winter in Japan. In other words, the high pressure area is extending over the west of Japan Islands and the low pressure area is extending over the east. Under the background of this location, the above observation showed the tendency that the wind direction changed slowly from north-west to north, and the wind speed rapidly increased approximately from 6m/s to 13m/s in 40∼50 minutes, and then changed slowly in the range approximately from 12m/s to 15m/s. On the other hand, 1/3 wave height gradually grew up to about 3.5 meters under the background that the wind speed increased and the wind direction changed slowly. The above data can be regarded to be the measurement of the wave development process, because wave height increases under the situation that the wind speed becomes faster and the wind direction does not change so much.

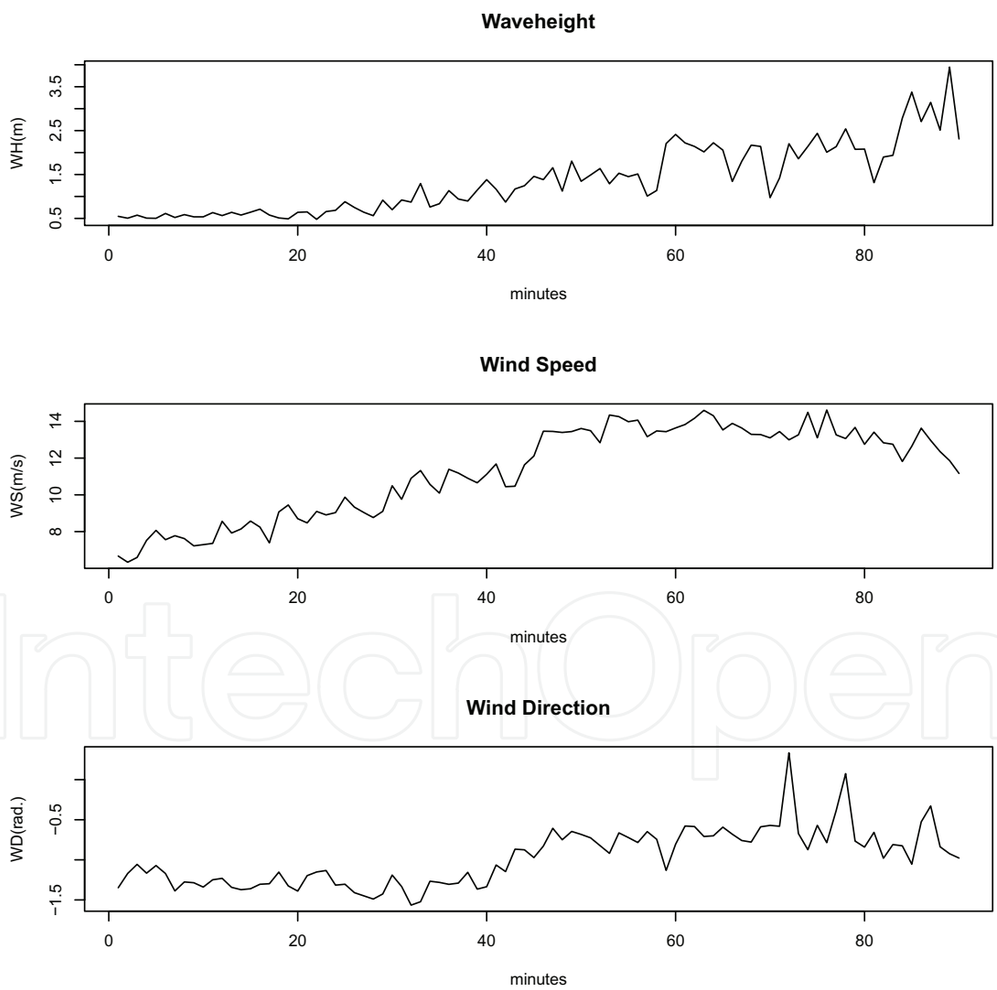

Fig. 2. Measured data on wave and wind (from the top, 1/3 significant wave height (m), wind speed (m/s), wind direction (rad.))

3.2 Some characteristics on the correlation structure

In the following, we make some preliminary analyses on the correlation structure of the measured data, in order to investigate what class of model is suitable for expressing the change of the measured data. In the following, let $\{WH_t\}$, $\{WS_t\}$ and $\{WD_t\}$ $(t = 1, \ldots, N)$ be sets of measurements of significant wave height, wind speed and wind direction, respectively, where t is the time point and N is the sample size.

3.2.1 Circular autocorrelation of the wind direction data

First, we invstigate the correlation structure of the directional time series data of wind direction. As a basic concept of exploratory circular data analysis, we refer to a book by Fisher (1993, Chapter 2) and use the following two transformations of WD_t

$$x_t = \cos(WD_t), \qquad y_t = \sin(WD_t) \tag{1}$$

In order to explore the possibility of detecting changes of direction, we use two statistics; one is the cumulative sum (CUSUM) plot displayed by the points

$$C_t = \sum_{i=1}^{t} x_i, \qquad S_t = \sum_{i=1}^{t} y_i \tag{2}$$

and the other is the cumulative mean direction plot $\{\Theta_t^c; t = 1, \ldots\}$, such that

$$\cos(\Theta_t^c) = C_t / \sqrt{C_t^2 + S_t^2}, \qquad \sin(\Theta_t^c) = S_t / \sqrt{C_t^2 + S_t^2} \tag{3}$$

are satisfied simultaneously. CUSUM plot is displayed in the left of Figure 3, where the horizontal axis denotes C_t and the vertical axis denotes S_t. Also, the cumulative mean directional plot is displayed in the right of Figure 3, where the horizontal axis denotes the time point t and the vertical axis denotes Θ_t^c. It is noted that the change in statistical structure of the directional time series data is admitted, when the trend of CUSUM plot is clearly different from the straight line whose slope is one, and when the value of the cumulative mean directional plot is clearly different from the constant value. The cumulative mean directional plot suggests the possibility that the directional time series data have a change point of statistical structure at $t = 40$ roughly, and in this case the time series exhibits nonstationarity. We also checked the statistical test of change in mean direction by using CircStats (Chapter 11 of Jammalamadaka and SenGupta (2001)). The result showed that there exists a change point at the time point $t = 42$, which suggested that the data exhibit nonstationarity.

Now we are interested in whether there is clear difference in the correlation structures, between the case when we regard the wind direction data to be circular time series data and the case when we regard the data to be linear time series data. For the estimation of correlation, it is necessary to subtract the trend of the data. Therefore, we estimate the trend from the following two standpoints. One is the esimation by regarding the data to be circular time series data. In this case, for estimating trend, we obtain the smoothed series of $\{x_t\}$ and $\{y_t\}$ by using the locally weighted regression (LOWESS). And then, based on the smoothed series, say $\{x_t^*\}$ and $\{y_t^*\}$, we obtain the smoothed trend of wind direction T_t^*, such that

$$\frac{x_t^*}{\sqrt{(x_t^*)^2 + (y_t^*)^2}} = \cos(T_t^*), \qquad \frac{y_t^*}{\sqrt{(x_t^*)^2 + (y_t^*)^2}} = \sin(T_t^*) \tag{4}$$

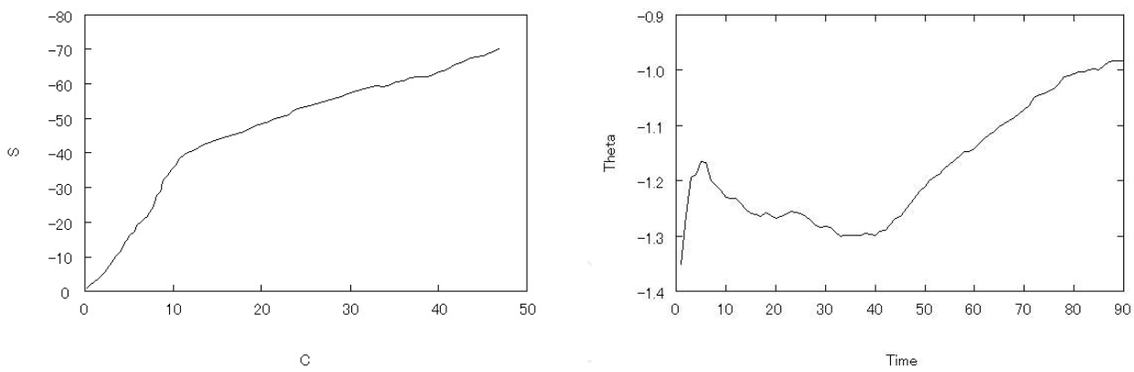

Fig. 3. Cumulative sum plot (left) and Cumulative mean directional plot (right)

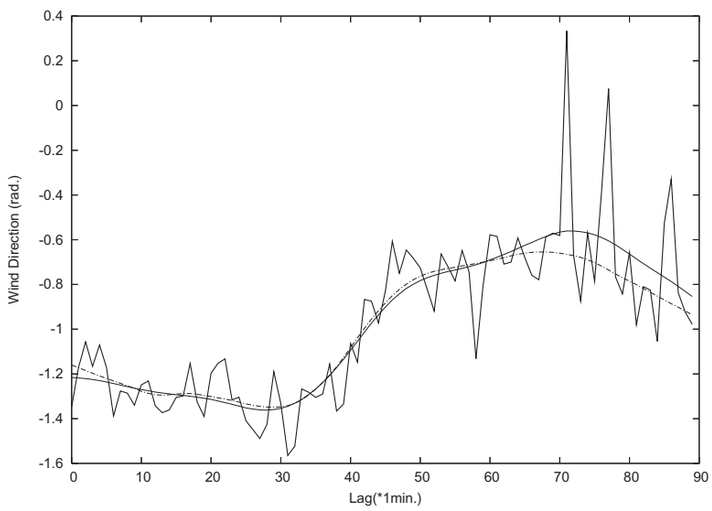

Fig. 4. Trend estimation on wind direction based on $\{T_t^*\}$ (dotted curve) and $\{T_t^{**}\}$ (solid curve)

are satisfied simultaneously. Another is the trend estimation based on linear time series data, which is given in Kitagawa and Gersch (1985). The trend of $\{WD_t\}$ can be obtained by applying the trend model,

$$WD_t = T_t^{**} + \zeta_t, \qquad \zeta_t \sim N(0, \sigma_\zeta^2) \tag{5}$$

and

$$T_t^{**} - T_{t-1}^{**} = v_t, \qquad v_t \sim N(0, \sigma_v^2) \tag{6}$$

where T_t^{**} is the random variable to express the trend, σ_ζ^2 and σ_v^2 are unknown variances of ζ_t and v_t, respectively. Figure 4 shows the trend estimation based on T_t^* and T_t^{**}, where the dotted curve means $\{T_t^*\}$ and the sold curve means $\{T_t^{**}\}$. It looks that there is no clear difference between $\{T_t^*\}$ and $\{T_t^{**}\}$. So we estimate circular autocorrelation coefficient based on the subtracted series, $WD_t^* \equiv WD_t - T_t^*$. Based on circular-circular association (Fisher

(1993, Chapter 6)), the sample circular autocorrelation coefficient is given by

$$\hat{\rho}^*(\tau) = \frac{4(A_\tau B_\tau - C_\tau D_\tau)}{\left[(N^2 - E_\tau^2 - F_\tau^2)(N^2 - G_\tau^2 - H_\tau^2)\right]^{1/2}}, \quad \tau = 0, 1, \ldots \tag{7}$$

where τ is the time lag, and

$$\begin{aligned} &A_\tau = \sum_{t=1}^{N-\tau} \cos WD_t^* \cos WD_{t+\tau}^*,\ B_\tau = \sum_{t=1}^{N-\tau} \sin WD_t^* \sin WD_{t+\tau}^*,\ C_\tau = \sum_{t=1}^{N-\tau} \cos WD_t^* \sin WD_{t+\tau}^*, \\ &D_\tau = \sum_{t=1}^{N-\tau} \sin WD_t^* \cos WD_{t+\tau}^*,\ E_\tau = \sum_{t=1}^{N-\tau} \cos(2WD_t^*),\ F_\tau = \sum_{t=1}^{N-\tau} \sin(2WD_t^*),\ G_\tau = \sum_{t=1}^{N-\tau} \cos(2WD_{t+\tau}^*), \\ &H_\tau = \sum_{t=1}^{N-\tau} \sin(2WD_{t+\tau}^*) \end{aligned} \tag{8}$$

On the other hand, the sample autocorrelation function of the time series data WD_t^* is given by

$$\begin{aligned} \hat{\rho}^{**}(\tau) &= \frac{\sum_{t=1}^{N-\tau}(WD_{t+\tau}^* - \overline{WD^*})(WD_t^* - \overline{WD^*})}{\sum_{t=1}^{N}(WD_t^* - \overline{WD^*})^2}, \\ \overline{WD^*} &= \frac{1}{N}\sum_{t=1}^{N} WD_t^* \end{aligned} \tag{9}$$

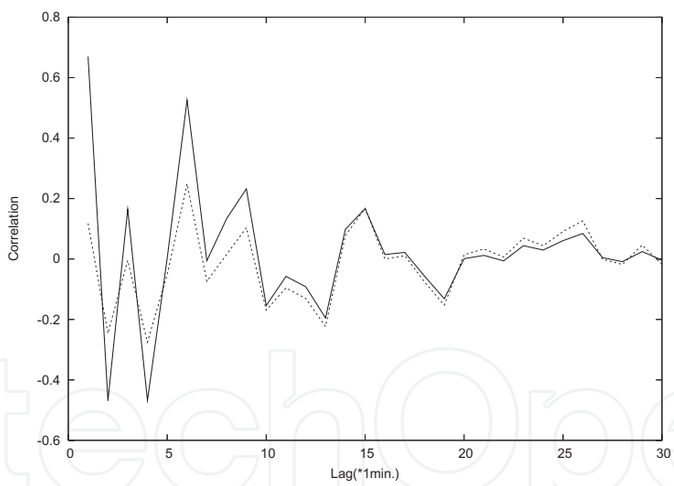

Fig. 5. Comparion between $\{\hat{\rho}^*(\tau)\}$ (bold line) and $\{\hat{\rho}^{**}(\tau)\}$ (dotted line)

Figure 5 displays the estimates of $\hat{\rho}^*(\tau)$ and $\hat{\rho}^{**}(\tau)$ ($0 \leq \tau \leq 30$), where the vertical axis denotes the correlation, the horizontal axis denotes τ in minutes, and the bold and dotted lines correspond to $\hat{\rho}^*(\tau)$ and $\hat{\rho}^{**}(\tau)$, respectively. We observe that they change similarly with the same tendency, although $|\hat{\rho}^*(\tau)|$ takes slightly larger values than $|\hat{\rho}^{**}(\tau)|$ when τ is small. It is evaluated from this result that the sample circular autocorrelation coefficient can be approximated by the linear correlation to some extent. Also, it suggests the possibility that it is sufficient to express the dynamic structure of the measured data by using the linear time series model.

Lag	(i)	(ii)	Lag	(i)	(ii)
0	0.038	0.084	11	0.174	0.173
1	-0.096	-0.085	12	0.156	0.184
2	0.102	0.093	13	0.183	0.228
3	0.006	-0.014	14	0.176	0.188
4	-0.227	-0.214	15	0.155	0.171
5	-0.139	-0.133	16	0.025	0.032
6	0.067	0.087	17	0.300	0.335
7	0.076	0.119	18	0.046	0.016
8	0.040	0.050	19	-0.080	-0.058
9	-0.139	-0.147	20	-0.070	-0.042
10	-0.039	-0.050			

Table 1. Cross correlation functions ((i) $\{WD_t\}$ and $\{WH_t\}$, (ii) $\{\sin(WD_t)\}$ and $\{WH_t\}$)

3.2.2 Cross correlation among wind speed, wind direction and wave height

Next, we focus on the cross correlations among $\{WS_t\}$, $\{WD_t\}$ and $\{WH_t\}$. We estimated the cross correlation function between $\{WH_t\}$ and the variables $\{WS_t\}$, $\{WD_t\}$ and $\{\sin(WD_t)\}$, by using the time series data after subtraction of their trends estimated by LOWESS method. Figure 6 shows an estimated result of the cross correlation function between $\{WS_t\}$ and $\{WH_t\}$ by using the sample cross correlation function $\gamma(\tau)$ ($\tau = 0, \pm 1, \ldots$),

$$\gamma(\tau) = \frac{\sum_{t=1}^{N-\tau}(WH_t - \overline{WH})(WS_{t+\tau} - \overline{WS})}{\sqrt{\sum_{t=1}^{N}(WH_t - \overline{WH})^2}\sqrt{\sum_{t=1}^{N}(WS_t - \overline{WS})^2}}, \quad \overline{WH} = \frac{1}{N}\sum_{t=1}^{N} WH_t, \ \overline{WS} = \frac{1}{N}\sum_{t=1}^{N} WS_t \tag{10}$$

where the horizontal means the time lag in minutes and two parallel lines denote Bartlett's bounds (i.e., $\pm 1.96N^{-1/2}$). It suggests the possibility that the change in wind speed affects the one of wave height after 10$\sim$20 minutes.

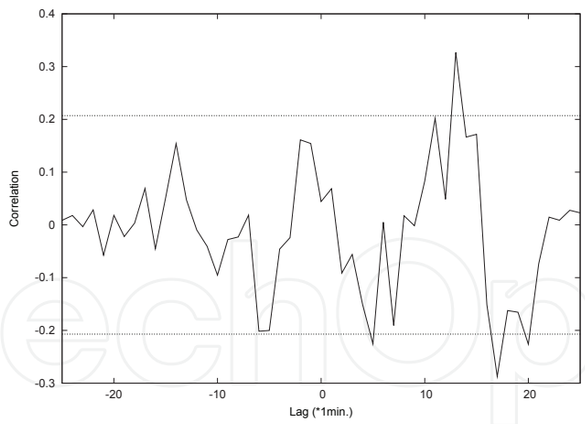

Fig. 6. Cross correlation function between $\{WS_t\}$ and $\{WH_t\}$ with Bartlett's bounds

For estimation of the correlation between $\{WD_t\}$ and $\{WH_t\}$, it is of interest how we treat the directional variable WD_t. Table 1 gives estimated values of the cross correlation functions in the two cases, (i) $\{WD_t\}$ and $\{WH_t\}$ and (ii) $\{\sin(WD_t)\}$ and $\{WH_t\}$. It is observed that the absolute value of (ii) tends to take larger values than the one of (i). This result suggests the possibility that it is expected to improve the prediction accuracy by adopting the variables $\sin(WD_t)$ (and $\cos(WD_t)$) as the explanatory variables, instead of using WD_t.

3.3 A statistical modeling on the change of wave height by wind forcing

Suppose that we predict the future values of wave height $\{WH_{N+l}; l = 1, \ldots, L\}$, based on the historical data $\{WH_t, WS_t, WD_t\}$ $(t = 1, \ldots, N)$. We start our consideration by assuming that the time series $\{WH_t\}$, $\{WS_t\}$ and $\{WD_t\}$ are stationary, after applying a proper transformation (the detail is described later in this section). We write the change of $\{WH_t\}$ as

$$WH_t = m_L + \sum_{i=1}^{p} \beta_i^{(1)} WH_{t-i} + \sum_{i=1}^{p}\sum_{k=1}^{K} \beta_{i,k}^{(3)} \cos(k \cdot WD_{t-i}) + \sum_{i=1}^{p}\sum_{k=1}^{K} \beta_{i,k}^{(4)} \sin(k \cdot WD_{t-i}) + \sum_{i=1}^{p} \beta_i^{(2)} WS_{t-i} + \varepsilon_t^{(1)}, \qquad \varepsilon_t^{(1)} \sim WN(0, \sigma_{WH}^2) \tag{11}$$

where p and K are orders, m_L is the unknown mean, β's are unknown weights, and $\varepsilon_t^{(1)}$ is the random variable which follows a white noise process with $E(\varepsilon_t^{(1)})$=0 and $V(\varepsilon_t^{(1)}) = \sigma_{WH}^2$. Similarly, we write

$$WS_t = m_S + \sum_{i=1}^{p} \gamma_i^{(1)} WH_{t-i} + \sum_{i=1}^{p}\sum_{k=1}^{K} \gamma_{i,k}^{(3)} \cos(k \cdot WD_{t-i}) + \sum_{i=1}^{p}\sum_{k=1}^{K} \gamma_{i,k}^{(4)} \sin(k \cdot WD_{t-i}) + \sum_{i=1}^{p} \gamma_i^{(2)} WS_{t-i} + \varepsilon_t^{(2)}, \qquad \varepsilon_t^{(2)} \sim WN(0, \sigma_{WN}^2) \tag{12}$$

and $\sin(h \cdot WD_t)$ and $\cos(h \cdot WD_t)$ $(h = 1, \ldots, K)$ as

$$\sin(h \cdot WD_t) = m_h + \sum_{i=1}^{p} \delta_i^{(1)} WH_{t-i} + \sum_{i=1}^{p}\sum_{k=1}^{K} \delta_{i,k}^{(3)} \cos(k \cdot WD_{t-i}) + \sum_{i=1}^{p}\sum_{k=1}^{K} \delta_{i,k}^{(4)} \sin(k \cdot WD_{t-i}) + \sum_{i=1}^{p} \delta_i^{(2)} WS_{t-i} + \delta_t^{(h)}, \qquad \delta_t^{(h)} \sim WN(0, \sigma_h^2) \tag{13}$$

and so forth, where m_s, m_h, γ's and δ's are unknown weights. Put the state vector at time t by

$$\boldsymbol{y}_t^{(K)} \equiv (WH_t, WS_t, \cos(WD_t), \sin(WD_t), \ldots, \cos(K \cdot WD_t), \sin(K \cdot WD_t))' \tag{14}$$

Then we can write

$$\boldsymbol{y}_t^{(K)} = \boldsymbol{m}^{(K)} + A_1^{(K)} \boldsymbol{y}_{t-1}^{(K)} + \cdots + A_p^{(K)} \boldsymbol{y}_{t-p}^{(K)} + \boldsymbol{\delta}_t^{(K)}, \quad \boldsymbol{\delta}_t^{(K)} \sim WN(\mathbf{0}, \Sigma^{(K)}) \tag{15}$$

where $\boldsymbol{m}^{(K)}$ is the unknown mean vector, $A_i^{(K)}$ $(i = 1, \ldots, p)$ is the unknown coefficient matrix, and $\boldsymbol{\delta}_t^{(K)}$ follows the multivariate white noise process with mean $\mathbf{0}$ and the dispersion matrix $\Sigma^{(K)}$. This is a multivariate vector autoregressive model of the pth order, and therefore, the estimates for elements of unknown matrices $A_i^{(K)}$ can be obtained by using the least squares method (e.g., Brockwell and Davis (1996)). Thus, we can construct an l-step $(l = 1, \ldots, L)$ ahead predictor based on (15) by

$$\hat{\boldsymbol{y}}_{N+l}^{(K)} = \hat{\boldsymbol{m}}^{(K)} + \hat{A}_1^{(K)} \boldsymbol{z}_{N+l-1}^{(K)} + \hat{A}_2^{(K)} \boldsymbol{z}_{N+l-2}^{(K)} + \cdots + \hat{A}_p^{(K)} \boldsymbol{z}_{N+l-p}^{(K)} \tag{16}$$

and $\boldsymbol{z}_{N+l-m}^{(K)} = \boldsymbol{y}_{N+l-p}^{(K)}$ $(l \leq p)$, $\boldsymbol{z}_{N+l-m}^{(K)} = \hat{\boldsymbol{y}}_{N+l-p}^{(K)}$ $(l > p)$, where $\hat{A}_i$ is the least squares estimator of A_i, The predicted values of WH_{N+l} $(l = 1, \ldots, L)$ can be obtained from the prediction of $\hat{\boldsymbol{y}}_{N+l}^{(K)}$.
However, the model (15) with the state vector (14) has a drawback in computational aspect. It is probable that the accuracy of the estimates of parameter becomes worse when both K and p become large, because (15) has $(2 + 2K) + p(2 + 2K)^2$ unknown parameters to be estimated. For improving the prediction accuracies, the dimension of the state vector $\hat{\boldsymbol{y}}_t^{(K)}$ should be small. In order to taking account of the multiple directional information with the small numbers of variables, we focus on the following linear sum

$$\widetilde{WD}_t^{(K)} \equiv \omega_1 \cos(WD_t) + \omega_2 \sin(WD_t) + \cdots + \omega_{2K-1} \cos(K \cdot WD_t) + \omega_{2K} \sin(K \cdot WD_t) \quad (17)$$

where ω_i $(i = 1, \ldots, 2K)$ are unknown weights. And we propose to use the model (15) with the state vector

$$\tilde{\boldsymbol{y}}_t^{(K)} \equiv (WH_t, WS_t, \widetilde{WD}_t^{(K)})' \quad (18)$$

Here, it is necessary to determine the optimum order K and the value of ω_i. For determining ω_i, we introduce the concept of principal component analysis. $\widetilde{WD}_t^{(K)}$ can be written as

$$\widetilde{WD}_t^{(K)} = \Omega_K' D_t^{(K)} \quad (19)$$

where $\Omega_K = (\omega_1, \ldots, \omega_{2K})'$ and $D_t^{(K)} = (\cos(WD_t), \sin(WD_t), \ldots, \cos(K \cdot WD_t), \sin(K \cdot WD_t))'$.
We select the values of Ω_K so that

$$V(\widetilde{WD}_t^{(K)}) = \Omega_K' \Sigma_t^{(K)} \Omega_K \quad (20)$$

is maximized under the constraints $\Omega_K' \Omega_K = 1$, where $\Sigma_t^{(K)}$ is the dispersion matrix of $D_t^{(K)}$. Ω_K can be obtained as the eigenvector $b^{(K)}$ of the eigen equation,

$$\Sigma_t^{(K)} b^{(K)} = \lambda b^{(K)} \quad (21)$$

Let $\lambda_1 \geq \cdots \geq \lambda_{2K}$ be $2K$ eigenvalues of the eigen equation. We choose the eigenvector which corresponds to λ_1 with unit norm, say $\tilde{b}_M^{(K)}$, with K fixed. We estimate $\widetilde{WD}_t^{(K)}$ by

$$\widehat{\widetilde{WD}}_t^{(K)} = \tilde{b}_M^{(K)} D_t^{(K)} \quad (22)$$

As for the selection of the order K, we choose the value of K such that the squared sum of the prediction errors,

$$S_l(K) = \frac{1}{N - l - N^* + 1} \sum_{t=N^*}^{N-l} (WH_{t+l} - \widehat{WH}_{t+l}^{(K)})^2 \quad (23)$$

is minimized for every l, where $\widehat{WH}_{t+l}^{(K)}$ is the predicted value by (16) and N^* is a prefixed value. For selection of p in (15), we use AIC (Akaike Information Criterion), under the value of K is fixed.

As observed in Figure 2, the time series data of WH_t, WS_t and WD_t during the wave development process exhibit nonstationarity. We follow the method of ARIMA model by Box and Jenkins (1976) and focus on the differenced time series. In other words, we regard the differenced series to be stationary and then fit

$$\boldsymbol{x}_t^{(K)} = B_1^{(K)}\boldsymbol{x}_{t-1}^{(K)} + \cdots + B_p^{(K)}\boldsymbol{x}_{t-p}^{(K)} + \boldsymbol{\epsilon}_t^{(K)}, \qquad \boldsymbol{\epsilon}_t^{(K)} \sim WN(\mathbf{0}, \Sigma_{\boldsymbol{\epsilon}^{(K)}}) \tag{24}$$

and

$$\boldsymbol{x}_t^{(K)} \equiv (\nabla WH_t, \nabla WS_t, \nabla \widehat{\widehat{WD}}_t^{(K)})', \tag{25}$$

where ∇ is the back-shift operator such that $\nabla WH_t = WH_t - WH_{t-1}$.

3.4 The effect of angular-linear structure on the prediction of wave height

In the following, we examine the availability of the proposed method through the evaluation of the prediction accuracy on wave height. For this purpose, we carried out the numerical experiments on prediction accuracy by using the measured data shown in Figure 2. The procedure of the prediction experiment is as follows. First, we fit the model (24) to the multivariate time series data $\{WH_t, WS_t, WD_t; t = 1\ldots, 50\}$ and then obtain the prediction values of WH_t up to 5 steps ahead (1 step corresponds to 1 minute). Next, we fit the model to the time series data from t=2 to t=51 and obtain the predicted values in the same way. After repeating this procedure, the prediction accuracy is evaluated based on the predicted values and realizations. As criteria for evaluation, we define the mean absolute error (MAE) and the correlation coefficient (COR) by

$$\mathrm{MAE}(l) \equiv \frac{1}{M}\sum_{i=1}^{M} |WH_{N+l}^{(i)} - \widehat{WH}_{N+l}^{(i)}| \tag{26}$$

$$\mathrm{COR}(l) \equiv \frac{\sum_{i=1}^{M}(WH_{N+l}^{(i)} - \overline{WH}^{(i)}(l))(\widehat{WH}_{N+l}^{(i)} - \overline{\widehat{WH}}^{(i)}(l))}{\sqrt{\sum_{i=1}^{M}(WH_{N+l}^{(i)} - \overline{WH}^{(i)}(l))^2}\sqrt{\sum_{i=1}^{M}(\widehat{WH}_{N+l}^{(i)} - \overline{\widehat{WH}}^{(i)}(l))^2}},$$

$$\overline{WH}(l) = \frac{1}{M}\sum_{i=1}^{M} WH_{N+l}^{(i)}, \ \overline{\widehat{WH}}(l) = \frac{1}{M}\sum_{i=1}^{M} \widehat{WH}_{N+l}^{(i)} \tag{27}$$

where l is the prediction step ($l = 1, \ldots, 5$), $WH_t^{(i)}$ is the realization of WH_t at the ith experiment, $\widehat{WH}_t^{(i)}$ is the predicted value of WH_t at the ith experiment, and M is the number of repetitions of the experiment. MAE gives better evaluation as the predicted value gets closer to the observation. COR is defined as the sample correlation between the observations and predicted values, in order to evaluate the degree of accordance to their trends.

We first investigate whether the angular-linear structure of the proposed model give the positive effect on the prediction accuracy of wave height. For this purpose, we analyze whether it is possible to improve the prediction accuracy by taking into account the variables $\{\sin(k \cdot WD_t), \cos(k \cdot WD_t)\}$ $(k = 1, \ldots, K)$, instead of using the variable WD_t directly. In this experiment, we compare the prediction accuracy by using the model (24), under assuming the following three state vectors. The first is the vector consisted from the difference of WH_t, WS_t and WD_t,

$$\boldsymbol{x}_t \equiv (\nabla WH_t, \nabla WS_t, \nabla WD_t)' \tag{28}$$

	MAE					COR				
p	L=1	L=2	L=3	L=4	L=5	L=1	L=2	L=3	L=4	L=5
1	0.385	0.446	0.517	0.490	0.585	0.501	0.335	0.200	0.360	0.205
2	0.394	0.454	0.464	0.490	0.582	0.450	0.292	0.258	0.366	0.201
3	0.415	0.500	0.482	0.474	0.601	0.346	0.195	0.159	0.403	0.155
4	0.428	0.518	0.505	0.487	0.613	0.322	0.123	0.081	0.357	0.152
5	0.421	0.528	0.494	0.493	0.604	0.333	0.093	0.063	0.320	0.156

Table 2. Prediction accuracy by using the model (24) with the state vector (28) (M=35)

	MAE					COR				
p	L=1	L=2	L=3	L=4	L=5	L=1	L=2	L=3	L=4	L=5
1	0.360	0.480	0.506	0.552	0.589	0.492	0.291	0.208	0.389	0.221
2	0.357	0.473	0.502	0.544	0.573	0.483	0.281	0.188	0.333	0.154
3	0.362	0.477	0.508	0.550	0.598	0.465	0.255	0.145	0.258	-0.078
4	0.356	0.474	0.502	0.540	0.586	0.479	0.260	0.146	0.312	-0.007
5	0.372	0.492	0.506	0.539	0.590	0.442	0.207	0.130	0.285	0.015

Table 3. Prediction accuracy by using the model (24) with the state vector (29) (M=35)

	MAE					COR				
p	L=1	L=2	L=3	L=4	L=5	L=1	L=2	L=3	L=4	L=5
1	0.378	0.445	0.490	0.485	0.600	0.481	0.338	0.234	0.370	0.163
2	0.353	0.435	0.456	0.502	0.574	0.433	0.296	0.259	0.360	0.180
3	0.367	0.440	0.478	0.493	0.575	0.380	0.256	0.174	0.381	0.146
4	0.367	0.446	0.473	0.480	0.571	0.384	0.258	0.178	0.396	0.173
5	0.365	0.439	0.475	0.488	0.576	0.381	0.260	0.171	0.387	0.147

Table 4. Prediction accuracy by using the model (24) with the state vector (25) (M=35, K=25)

The second is

$$\boldsymbol{x}_t \equiv (\nabla WH_t, \nabla WS_t, \nabla \cos(WD_t), \nabla \sin(WD_t))' \tag{29}$$

And the third is (25), the proposed method.

Tables 2, 3 and 4 show MAE's and COR's in the above three cases, respectively. It is noted that each experiment was carried out under the condition that the order p was fixed in the range from 1 to 5. Overall, the result by using (29) tends to give smaller MAE's than the one by using (28). It suggests the possibility that taking into account the angular-linear structure is effective for improving the prediction accuracies by the predictor based on (28). The result of COR also shows the similar tendency. It is noted that, as the order p and the prediction step L are larger, the prediction accuracy based on (29) becomes worse to take negative correlations. The prediction based on the model with the state vector (25) tends to give the best prediction accuracy among the three models. This suggests that the principal component structure of (25) worked effectively, which contributed to the improvement of the prediction accuracy.

4. Predicting the change of wave height from surface wind

In the previous section, we developed a statistical model for explaining the dynamic relationship between ocean wind and wave height. Now we consider the prediction problem on wave height based on the motion of the surface wind, observed by ground-based observation. For this purpose, we develop a new method by applying the model presented in the previous section. Also, in order to evaluate the availability of the developed model, we compare the prediction accuracies between the proposed model and traditional time series models.

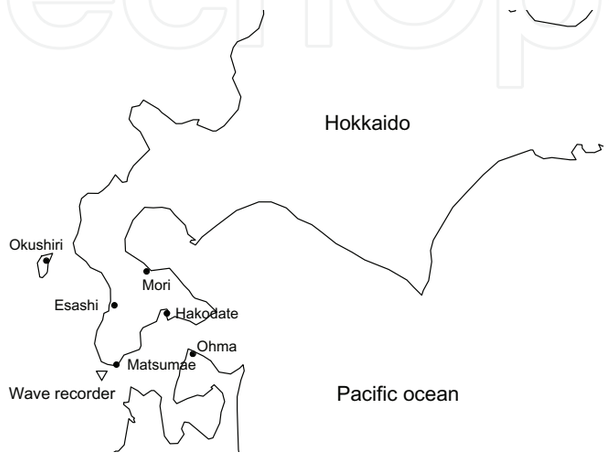

Fig. 7. Locations of the sensor for ultrasonic wave height meter (inverted triangle) and major AMeDAS stations around the sensor (black circles)

4.1 Ground-based observation on surface wind and measurement of wave height

In Japan, as described in Introduction, many stations of AMeDAS and the sensors for ultrasonic wave height meters have been located in various regions and coastal areas of this country by the Japan Meteorological Agency. In the following, we consider a case study on prediction of the wave height in Matsumae-oki, the sea area in the southwest of Hokkaido. Figure 7 shows a map of the locations of the sensor of a wave height meter in Matsumae-oki (42°24′38″N, 140°05′50″E) and major AMeDAS stations located around the sensor. The monitoring of the changes of wind speed and wind direction, and the measurement of wave height are carrying out constantly, and the measured data are available via Internet. For the following analysis, we obtained the dataset of wave height measured in Matsumae-oki and the datasets of wind speed and wind direction monitored at the AMeDAS station in Matsumae-cho, which is located roughly 5 km away from the measuring point of wave height. Figure 8 displays the changes in the significant wave height (m) measured in Matsumae-oki, and wind speed (m/s) and wind direction (rad.) monitored in Matsumae-cho, which were measured every hour on the hour. They are the records for every four seasons in the period from April 2010 to February 2011. As the datasets for four seasons, we obtained the measured data in the period from Apr. 1 to May 31 for spring, Jul. 1 to Aug. 31 for summer, Oct. 1 to Nov. 31 for autumn and Jan. 1 to Feb. 28 of 2011 for winter. The measured data on wind speed and wind direction are provided as the mean value over the past 10 minutes, and the measured data on 1/3 significant wave height is calculated based the sea surface data over

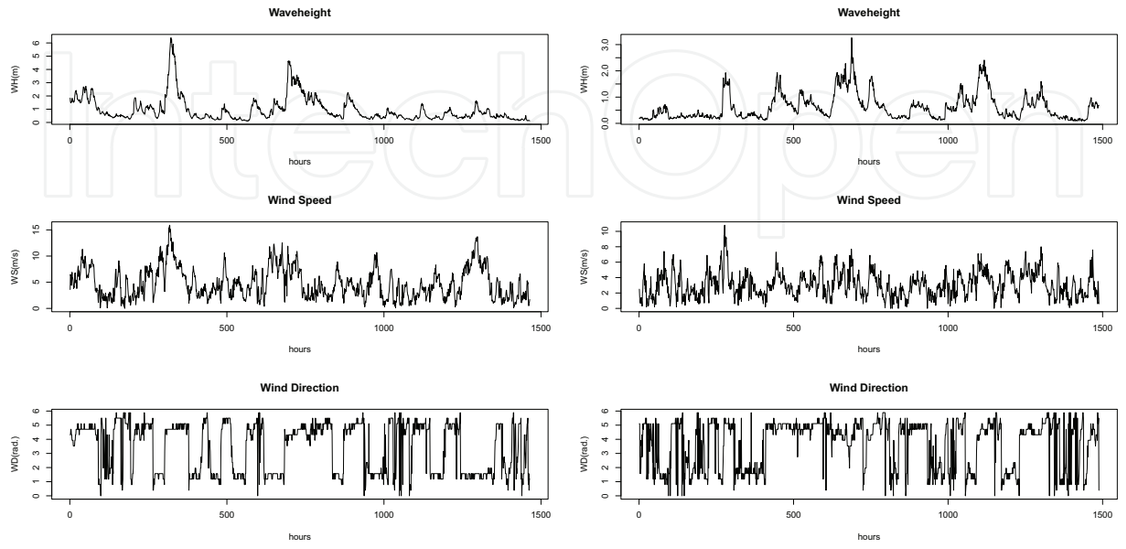

(a) Spring (Apr. 1- May 31)

(b) Summer (Jul. 1- Aug. 31)

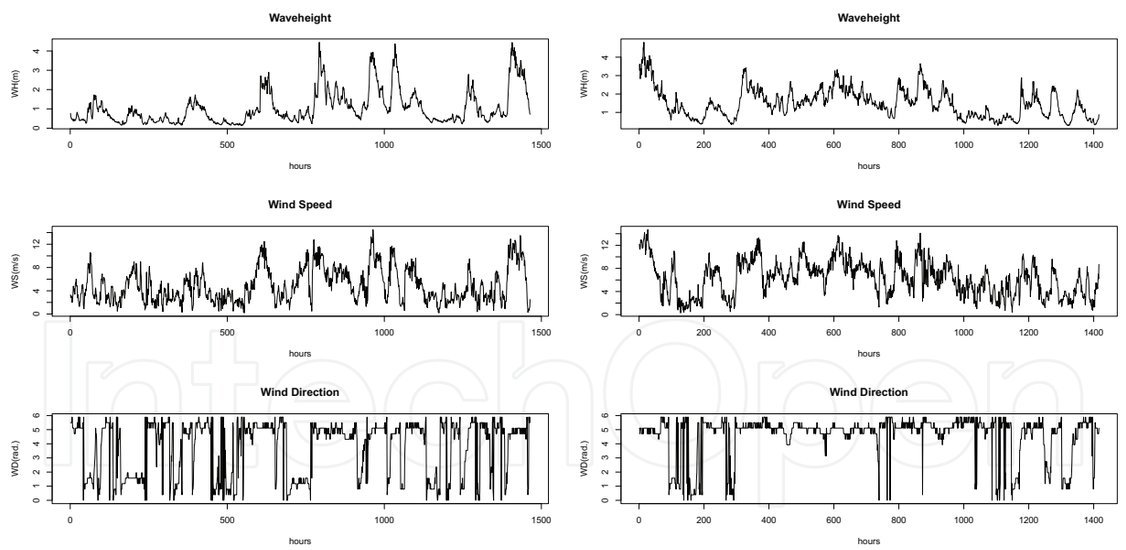

(c) Autumn (Oct. 1- Nov. 31)

(d) Winter (Jan. 1- Feb. 28)

Fig. 8. The changes of 1/3 significant wave height (m) (top), wind speed (m/s) (middle) and wind direction (rad.) (bottom) for four seasons (Apr. 2010 - Feb. 2011)

the past 25 minutes. It is noted that the origin of the wind direction data is defined to be north and the positive value means the clockwise direction.

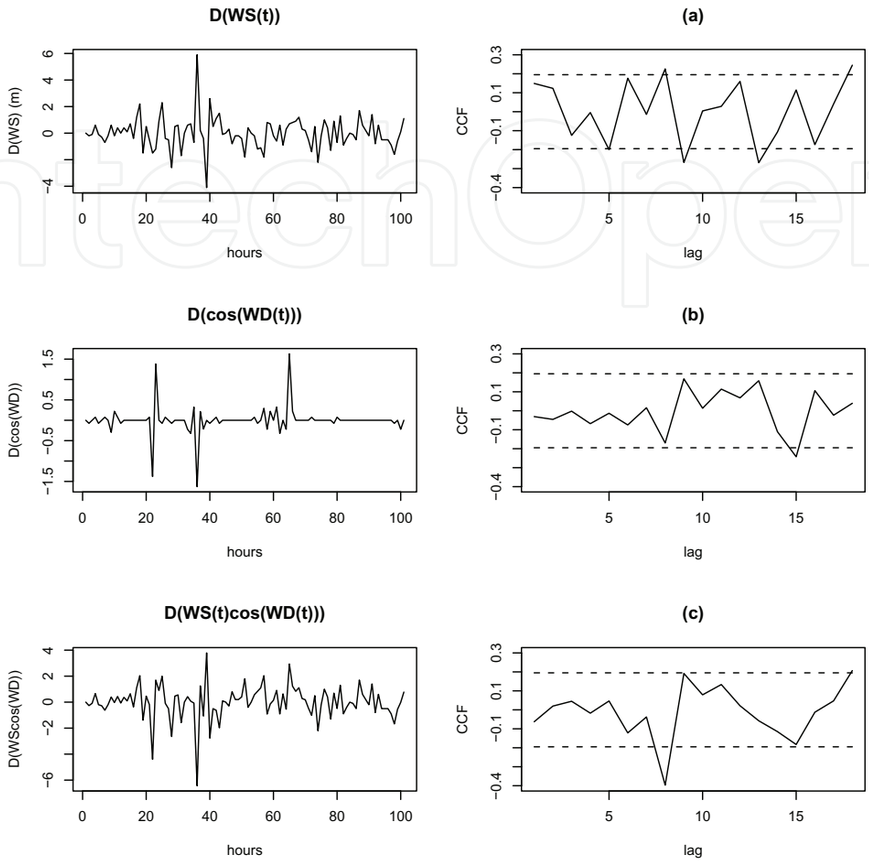

Fig. 9. Time series plots of $\{\nabla WS_t^*\}$, $\{\nabla \cos(WD^*{}_t)\}$, $\{\nabla(WS_t^* \cos(WD_t^*))\}$ (left column) and the cross correlation functions in the cases (a)-(c) (right column)

4.2 Cross correlation among the measured data

First, we consider how we treat the measured data of the wind direction. In the following, let $\{WS_t^*\}$ and $\{WD_t^*\}$ be the measured time series data on wind speed and wind direction of the surface wind.

Figure 9 shows the time series plots of $\{\nabla WS_t^*\}$, $\{\nabla \cos(WD_t^*)\}$ and $\{\nabla(WS_t^* \cos(WD_t^*))\}$, and the cross correlation functions in the 3 cases, (a) $\{\nabla WS_t^*\}$ and $\{\nabla WH_t\}$, (b) $\{\nabla \cos(WD_t^*)\}$ and $\{\nabla WH_t\}$, and (c) $\{\nabla(WS_t^* \cos(WD_t^*))\}$ and $\{\nabla WH_t\}$, which were estimated by (10), where the dotted lines mean the Bartlett's bounds. We observe that the case (c) gives larger cross correlation than the cases of (a) and (b).

4.3 Modeling the change of wave height by taking into account the change of surface wind

We consider a statistical model to express the change in wave height based on the change in surface wind, monitored at an AMeDAS station. Following the result in the previous section, we build a nonstationary time series model focusing on the change of $\nabla(WS_t^* \cos(WD_t^*))$. We write ∇WH_t as

$$\nabla WH_t = \sum_{i=1}^{p} \alpha_i \nabla WH_{t-i} + \sum_{i=1}^{p}\sum_{k=1}^{K} \beta_{i,k} \nabla (WS^*_{t-i} \cos(kWD^*_{t-i})) + \sum_{i=1}^{p}\sum_{k=1}^{K} \gamma_{i,k} \nabla (WS^*_{t-i} \sin(kWD^*_{t-i})) + \varepsilon_{1,t}, \ \ \varepsilon_{1,t} \sim WN(0, \sigma^2_{WH}) \tag{30}$$

where p and K are orders, (α, β, γ) are unknown coefficients and $\varepsilon_{1,t}$ is the random variable which follows a white noise process with $E(\varepsilon_{1,t})$=0 and $V(\varepsilon_{1,t}) = \sigma^2_{WH}$. Similarly, we write

$$\nabla (WS^*_t \sin(hWD^*_t)) = \sum_{i=1}^{p} \alpha^{(h)}_i \nabla WH_{t-i} + \sum_{i=1}^{p}\sum_{k=1}^{K} \beta^{(h)}_{i,k} \nabla (WS^*_{t-i} \cos(kWD^*_{t-i})) + \sum_{i=1}^{p}\sum_{k=1}^{K} \gamma^{(h)}_{i,k} \nabla (WS^*_{t-i} \sin(kWD^*_{t-i})) + \varepsilon^{(h)}_{2,t} \tag{31}$$

$$\nabla (WS^*_t \cos(hWD^*_t)) = \sum_{i=1}^{p} \alpha^{(h)}_i \nabla WH_{t-i} + \sum_{i=1}^{p}\sum_{k=1}^{K} \beta^{(h)}_{i,k} \nabla (WS^*_{t-i} \cos(kWD^*_{t-i})) + \sum_{i=1}^{p}\sum_{k=1}^{K} \gamma^{(h)}_{i,k} \nabla (WS^*_{t-i} \sin(kWD^*_{t-i})) + \varepsilon^{(h)}_{3,t} \tag{32}$$

for $h = 1, \ldots, K$, where $\varepsilon^{(h)}_{2,t} \sim WN(0, \sigma^2_{2,h})$ and $\varepsilon^{(h)}_{3,t} \sim WN(0, \sigma^2_{3,h})$.
Put the state vector at time point t by the (2K+1) dimensional vector

$$\boldsymbol{y}^{(K)}_t \equiv (\nabla WH_t, \ \nabla WC_1, \ \nabla WS_1, \ \ldots, \nabla WC_K, \ \nabla WS_K)' \tag{33}$$

where $WC_h = WS^*_t \cos(hWD^*_t)$ and $WS_h = WS^*_t \sin(hWD^*_t)$ $(h = 1, \ldots, K)$. Then the above models can be rewritten by a multivariate AR model,

$$\boldsymbol{y}^{(K)}_t = A^{(K)}_1 \boldsymbol{y}^{(K)}_{t-1} + \cdots + A^{(K)}_p \boldsymbol{y}^{(K)}_{t-p} + \boldsymbol{\delta}^{(K)}_t, \qquad \boldsymbol{\delta}^{(K)}_t \sim WN(\mathbf{0}, \Sigma^{(K)}) \tag{34}$$

where $A^{(K)}_i$ $(i = 1, \ldots, p)$ are unknown coefficient matrices and $\boldsymbol{\delta}^{(K)}_t$ follows the multivariate white noise process with mean $\mathbf{0}$ and the dispersion matrix $\Sigma^{(K)}$. An l-step ahead predictor can be constructed by

$$\hat{\boldsymbol{y}}^{(K)}_{N+l} = \hat{A}^{(K)}_1 \boldsymbol{z}^{(K)}_{N+l-1} + \hat{A}^{(K)}_2 \boldsymbol{z}^{(K)}_{N+l-2} + \cdots + \hat{A}^{(K)}_p \boldsymbol{z}^{(K)}_{N+l-p},$$
$$\boldsymbol{z}^{(K)}_{N+l-m} = \boldsymbol{y}^{(K)}_{N+l-p} (l \le p), \qquad \hat{\boldsymbol{y}}^{(K)}_{N+l-p} (l > p) \tag{35}$$

where $\hat{A}^{(K)}_i$ is the least squares estimator of $A^{(K)}_i$. Thus the l-step ahead predicted values, WH_{N+l} $(l = 1, \ldots, L)$, can be obtained by the predictor $\hat{\boldsymbol{y}}^{(K)}_{N+l}$.

	MAE					COR				
Model	L=1	L=2	L=3	L=4	L=5	L=1	L=2	L=3	L=4	L=5
(i)	0.114	0.167	0.222	0.242	0.267	0.982	0.955	0.927	0.886	0.862
(ii)	0.096	0.142	0.176	0.219	0.246	0.985	0.962	0.946	0.914	0.903
(iii)	0.103	0.143	0.178	0.215	0.239	0.984	0.960	0.944	0.912	0.903
(iv)	0.097	0.143	0.178	0.217	0.241	0.985	0.961	0.945	0.913	0.902
(v)	0.098	0.138	0.176	0.213	0.235	0.986	0.965	0.949	0.919	0.907

Table 5. MAE's and COR's based on spring data

4.4 Evaluation of the prediction accuracy

In the following, we evaluate the effectiveness of the proposed method by means of the prediction experiment which is similar to the one given in the subsection 3.4.
The procedure for the experiment is as follows. We select the time point to start prediction randomly in the range of the dataset. And then fit the proposed model to the measured time series data for 100 hours (i.e., sample size is 100), and obtain the predicted values up to 5 steps ahead (1 step corresponds to 1 hour). After repeating the procedures, we evaluate the prediction accuracy by MAE and COR. For evaluation of the prediction accuracy, we also obtain the predicted values when we used traditional time series models. The models introduced for comparison are defined as follows;
(i) $WH_t = \sum_{i=1}^{p} \alpha_i WH_{t-i} + \delta_{1,t}, \ \ \delta_{1,t} \sim WN(0, \sigma_1^2)$

(ii) $\nabla WH_t = \sum_{i=1}^{p} \beta_i \nabla WH_{t-i} + \delta_{2,t}, \ \ \delta_{2,t} \sim WN(0, \sigma_2^2)$

(iii) $\boldsymbol{y}_t = A_1 \boldsymbol{y}_{t-1} + \cdots + A_p \boldsymbol{y}_{t-p} + \boldsymbol{\delta}_{3,t}, \quad \boldsymbol{\delta}_t \sim WN(\mathbf{0}, \Sigma_{3,t}), \quad \boldsymbol{y}_t = (\nabla WH_t, \nabla WS_t^*)'$

(iv) $\boldsymbol{y}_t = B_1 \boldsymbol{y}_{t-1} + \cdots + B_p \boldsymbol{y}_{t-p} + \boldsymbol{\delta}_{4,t}, \quad \boldsymbol{\delta}_t \sim WN(\mathbf{0}, \Sigma_{4,t}), \quad \boldsymbol{y}_t = (\nabla WH_t, \nabla WS_t^* \cdot \nabla \cos(WD_t^*))'$

(v) $\boldsymbol{y}_t = C_1 \boldsymbol{y}_{t-1} + \cdots + C_p \boldsymbol{y}_{t-p} + \boldsymbol{\delta}_{5,t}, \quad \boldsymbol{\delta}_t \sim WN(\mathbf{0}, \Sigma_{5,t}), \quad \boldsymbol{y}_t = (\nabla WH_t, \nabla(WS_t^* \cos(WD_t^*)))'$

where $\{\alpha_i, \ \beta_i, \ A_i, \ B_i, \ C_i\}$ are unknown parameters. (i) and (ii) are univariate time series models based on wave height. The former is a stationary AR(p) model and the latter is a nonstationary ARIMA(p,1,0) model. (iii) is a multivariate AR model taking into account the wind speed as a covariate, and (iv) and (v) are multivariate AR models taking into account wind speed and wind direction as covariates. It is noted that if the changes of wind speed and wind direction are dependent, the prediction accuracy of (v) becomes better than that of (iv).
Table 5 shows MAE's and COR's of the above five models, based on the measured data in spring. The number of repetitions is 130. It is noted that we selected the order of the model by Akaike Information Criterion (AIC). By the comparison between (i) and (ii), we confirm that the nonstationary ARIMA model gives better prediction performance than the stationary AR model. Also, the comparisons between (ii) and (iii), (ii) and (iv), and (ii) and (v) show the tendency that the model taking into account the change of wind motion as covariate improves the prediction accuracy when we used the univariate time series model on wave height. Furthermore, the comparison between (iv) and (v) shows the tendency that the prediction accuracy by using (v) becomes better, which suggests that there exists the dependency between wind speed and wind direction.

(A) Spring

	MAE					COR				
Model	L=1	L=2	L=3	L=4	L=5	L=1	L=2	L=3	L=4	L=5
(i)	0.114	0.167	0.222	0.242	0.267	0.982	0.955	0.927	0.886	0.862
(ii)	0.096	0.142	0.176	0.219	0.246	0.985	0.962	0.946	0.914	0.903
(iii)	0.103	0.143	0.178	0.215	0.239	0.984	0.960	0.944	0.912	0.903
(iv)	0.097	0.143	0.178	0.217	0.241	0.985	0.961	0.945	0.913	0.902
(v)	0.098	0.138	0.176	0.213	0.235	0.986	0.965	0.949	0.919	0.907

(B) Summer

	MAE					COR				
Model	L=1	L=2	L=3	L=4	L=5	L=1	L=2	L=3	L=4	L=5
(i)	0.077	0.089	0.120	0.153	0.191	0.970	0.949	0.930	0.895	0.852
(ii)	0.074	0.085	0.106	0.136	0.155	0.980	0.974	0.959	0.929	0.896
(iii)	0.073	0.085	0.108	0.137	0.155	0.980	0.976	0.957	0.927	0.893
(iv)	0.072	0.081	0.107	0.136	0.156	0.981	0.977	0.958	0.927	0.892
(v)	0.072	0.083	0.105	0.132	0.149	0.981	0.975	0.959	0.930	0.897

(C) Autumn

	MAE					COR				
Model	L=1	L=2	L=3	L=4	L=5	L=1	L=2	L=3	L=4	L=5
(i)	0.094	0.169	0.235	0.293	0.327	0.984	0.937	0.903	0.837	0.789
(ii)	0.086	0.145	0.187	0.236	0.268	0.989	0.962	0.938	0.898	0.872
(iii)	0.083	0.144	0.188	0.231	0.259	0.990	0.964	0.940	0.901	0.875
(iv)	0.088	0.149	0.191	0.238	0.264	0.989	0.962	0.939	0.900	0.873
(v)	0.085	0.146	0.188	0.233	0.259	0.989	0.963	0.940	0.899	0.874

(D) Winter

	MAE					COR				
Model	L=1	L=2	L=3	L=4	L=5	L=1	L=2	L=3	L=4	L=5
(i)	0.107	0.168	0.234	0.266	0.301	0.979	0.948	0.905	0.873	0.828
(ii)	0.103	0.163	0.208	0.245	0.273	0.979	0.951	0.916	0.891	0.854
(iii)	0.103	0.156	0.202	0.243	0.271	0.979	0.952	0.916	0.890	0.852
(iv)	0.106	0.163	0.208	0.245	0.273	0.976	0.947	0.909	0.886	0.848
(v)	0.100	0.156	0.203	0.243	0.272	0.980	0.952	0.917	0.889	0.851

Table 6. Comparisons of MAE and COR for every season (Apr. 2010 - Feb. 2011)

4.5 Robustness on the predictability of wave height for every season

It is also of interest whether or not the effectiveness in prediction using the developed model is robust throughout a year. In Japan, there exists unique characteristics on the pressure pattern for every season. Therefore, it is necessary to investigate whether the model has the ability to improve the prediction accuracies by traditional models, for all seasons of a year.

Table 6 shows MAE's and COR's obtained by using the measured time series data for four seasons in the period from April 2010 to February 2011. Overall, the result has the tendency that the proposed model (v) has the ability to give the best prediction accuracy among the five models, although the degree on improvement of the accuracy are different for every season.

5. Conclusion

Our goal in this chapter is the development of a statistical approach for predicting the change of wave height, based on the measured data of the surface wind obtained by ground-based

observation. In section 3, we presented a method for predicting the change of wave height based on ocean wind, which was proposed by Hokimoto and Shimizu (2008). And in section 4, we developed a model for predicting the wave height from the change of surface wind, by applying the model given in the previous section. The evaluation on the prediction accuracy suggested the possibility that the method proposed in section 4 improves the prediction accuracies by using the predictors based on traditional time series models. As described at the beginning, the physical factors which impacts on the change in the sea state will change with correlations on space and time. At the present, the models presented in this chapter do not have spatial structure. For example, the development of the model, taking into account the directional change of the wind direction observed at multiple AMeDAS stations, will be available for deeper understandings on the dynamic interaction between the motions of wind and wave.

6. References

Athanassoulis, G.A., Stefanakos, C.N. (1995). A nonstationary stochastic model for long-term time series of significant wave height, *Journal of Geophysical Research*, 100(C8), 16149-16162.

Bollerslev, T.(1986). Generalized Autoregressive Conditional Heteroskedasticity, *Journal of Econometrics*, 31, 307-327.

Box, G.E.P., Jenkins, G.M. (1976). *Time Series Analysis, Forecasting and Control* (revised edition), Holden-Day, San Francisco.

Brockwell, P.J., Davis, R.A. (1996). *Introduction to Time Series and Forecasting*, Springer-Verlag, New York.

Brown, B.G., Katz, R.W., Murphy A.H. (1984). Time series models to simulate and forecast wind speed and wind power, *Journal of Climate and Applied Meteorology*, 23, 1184-1195.

Cunha C, Guedes S.C. (1999). On the choice of data transformation for modelling time series of significant wave height, *Ocean Eng*, 26, 489-506.

Daniel, A.R., Chen, A.A. (1991). Stochastic simulation and forecasting of hourly average wind speed sequences in Jamaica, *Sol Energy*, 46(1), 1-11.

Fisher, N.I. (1993). *Statistical Analysis of Circular Data*, Cambridge University Press, Cambridge.

Fisher, N.I., Lee, A. J. (1992). Regression models for an angular response, *Biometrics*, 48, 665-677.

Johnson, R.A., Wehrly, T.E. (1978). Some Angular-Linear Distributions and Related Regression Models, *Journal of the American Statistical Association*, 73, 602-606.

Hokimoto, T., Kimura, N., Iwamori, T., Amagai, K., Huzii, M. (2003). The effects of wind forcing on the dynamic spectrum in wave development: A statistical approach using a parametric model, *Journal of Geophysical Research*, 108(C10), 5-1-5-12.

Hokimoto, T., Shimizu, K. (2008). An angular-linear time series model for wave height prediction, *Ann Inst Stat Math*, 60, 781-800.

Kitagawa, G., Gersch, W. (1985). A Smoothness Priors Time-Varying AR Coefficient Modeling of Nonstationary Covariance Time Series, *IEEE Transactions on Automatic Control*, 30, 48-56.

Mardia, K.V., Jupp, P.E. (2000). *Directional Statistics*, John Wiley, New York.

O' Carroll (1984). Weather modelling for offshore operations, *The Statistician*, 33, 161-169.

Pierson, W.J., Neumann, G, and James, R.W. (1960). Practical Methods for Observing and Forecasting Ocean Waves By Means of Wave Spectra and Statistics, *U.S. Navy Hydrographic Office*, Reprint edition.

SenGupta, A. (2004). On the constructions of probability distributions for directional data, *Bulletin of the Calcutta Mathematical Society*, 96(2), 139-154.

SenGupta, A., Ugwuowo, F.I. (2006). Asymmetric circular-linear mutilvariate regression models with application to environmental data, *Environmental and Ecological Statistics*, 13, 299-309.

Stefanakos, C.N., Athanassoulis, G.A., Barstow, S.F. (2002). Mutivariate time series modelling of significant wave height, *Proceedings of International Society of Offshore and Polar Engineers Conference*, III, 66-73.

Sverdrup, H.U., Munk, W.H. (1947). Wind sea and swell: Theory of relation for forecasting, *U.S. Navy Hydrographic Office, Washington, D.C.*, No.601.

Walton, T. L., Borgman, L.E. (1990). Simulation of non-stationary, non-gaussian water levels on the great lakes, *Journal of the ASCE*, Waterway Port, Coastal, and Ocean Engineering Division, 116(6), 664-685.

Yim, J.Z., Chou, C., Ho, P. (2002). A study on simulating the time series of siginificant wave height near the keelung harbor, *Proceedings of International Society of Offshore and Polar Engineers Conference*, III, 92-96.

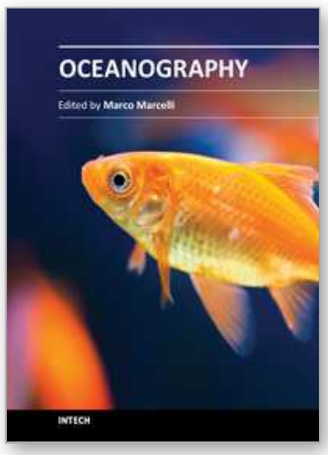

Oceanography

Edited by Prof. Marco Marcelli

ISBN 978-953-51-0301-1
Hard cover, 348 pages
Publisher InTech
Published online 23, March, 2012
Published in print edition March, 2012

How inappropriate to call this planet Earth when it is quite clearly Ocean (Arthur C. Clarke). Life has been originated in the oceans, human health and activities depend from the oceans and the world life is modulated by marine and oceanic processes. From the micro-scale, like coastal processes, to macro-scale, the oceans, the seas and the marine life, play the main role to maintain the earth equilibrium, both from a physical and a chemical point of view. Since ancient times, the world's oceans discovery has brought to humanity development and wealth of knowledge, the metaphors of Ulysses and Jason, represent the cultural growth gained through the explorations and discoveries. The modern oceanographic research represents one of the last frontier of the knowledge of our planet, it depends on the oceans exploration and so it is strictly connected to the development of new technologies. Furthermore, other scientific and social disciplines can provide many fundamental inputs to complete the description of the entire ocean ecosystem. Such multidisciplinary approach will lead us to understand the better way to preserve our "Blue Planet": the Earth.

How to reference

In order to correctly reference this scholarly work, feel free to copy and paste the following:

Tsukasa Hokimoto (2012). Prediction of Wave Height Based on the Monitoring of Surface Wind, Oceanography, Prof. Marco Marcelli (Ed.), ISBN: 978-953-51-0301-1, InTech, Available from: http://www.intechopen.com/books/oceanography/prediction-of-wave-height-based-on-the-monitoring-of-surface-wind

INTECH
open science | open minds

InTech Europe
University Campus STeP Ri
Slavka Krautzeka 83/A
51000 Rijeka, Croatia
Phone: +385 (51) 770 447
Fax: +385 (51) 686 166
www.intechopen.com

InTech China
Unit 405, Office Block, Hotel Equatorial Shanghai
No.65, Yan An Road (West), Shanghai, 200040, China
中国上海市延安西路65号上海国际贵都大饭店办公楼405单元
Phone: +86-21-62489820
Fax: +86-21-62489821

IntechOpen